

LIGHT WAVE TRANSFORMATION

PACS numbers: 42.25.Bs; 42.70.Qs; 73.20.Mf
DOI: 10.1070/QE2015v045n11ABEH015793

Efficiency of surface plasmon excitation at the photonic crystal–metal interface

T.I. Kuznetsova, N.A. Raspopov

Abstract. **We report the results of a theoretical investigation of light wave transformation in a one-dimensional photonic crystal. The scheme considered comprises an incident wave directed in parallel with layers of the photonic crystal under an assumption that the wave vector is far from a forbidden zone. Expressions for propagating and evanescent electromagnetic waves in a periodic medium of the photonic crystal are obtained. It is found that the transverse structure of the propagating wave comprises a strong constant component and a weak oscillating component with a period determined by that of the photonic crystal. On the contrary, the dependence of evanescent waves on transverse coordinates is presented by a strong oscillating component and a weak constant component. The process of transformation of propagating waves to evanescent waves at a crystal–metal interface is investigated. Parameters of the photonic crystal typical for synthetic opals are used in all numerical simulations. The theoretical approach elaborated yields in an explicit form the dependence of the amplitude of a generated surface wave on the period of the dielectric function modulation in the photonic crystal. The results obtained show that in the conditions close to plasmon resonance the amplitude of the surface wave may be on the order of or even exceed that of the initial incident wave.**

Keywords: *photonic crystal, evanescent waves, wave transformation at a crystal–metal interface, surface wave amplitude.*

1. Introduction

Classical methods for exciting surface plasmon polaritons (SPPs) at a metal–dielectric interface, described in fundamental work [1], are still used in experiments. These methods are based on the effect of frustrated total internal reflection or on the employment of metal periodic structures. In the last decade, investigations related to the search for other ways and schemes for obtaining SPPs have been actively developed. There are many schemes, in which light is directed to an ultranarrow channel in a metal layer or to a sub-wavelength hole or sub-micron slit in a thin metal film. Surface waves were then observed at the opposite side of the metal layer [2–4]. Phenomena occurring in this case were analysed theoretically by some authors (see, for example, [5–7] and review [8]). Of particular interest is the scheme [9], in which a light beam passed to a system of multiple holes in a metal film. This work has inspired numerous experimental and theoretical investigations (see, e.g., [10–12]).

Currently, there is a trend for combining plasmonics and specific features of photonic crystals. A rapidly developing field of studies has emerged, aimed at analysing new optical phenomena in photonic crystals and their practical employment. Relevant physical problems, some practical applications and possible prospects are discussed in [13–15]. These works combining plasmonics and photonic crystals pay much attention to modification of optical properties in crystals placed near a metal surface or comprising embedded metal particles. These phenomena were first studied and analysed in 1D photonic crystals [16–23]. These works studied the modification of the crystal zone structure caused by the interaction of Bloch waves with electromagnetic oscillations in metal and paid special attention to the role of forbidden photonic zones. It was asserted that the existence of surface plasmons is ensured by evanescent waves pertaining to forbidden zones of the photonic crystal. This statement was stressed in [17, 18].

In [24–29] and papers cited therein, experiments were performed with 2D and 3D photonic opal-like crystals. In one such experiment, two samples of different photonic crystals were used simultaneously. In some other experiments, a metal film deposited on a glass substrate (or directly on the crystal surface) was used. The metal film added to the system implemented the conditions for the existence of plasmons which resulted in a drastic change of the total transmission and reflection coefficients with a complicated angular structure of these coefficients. The angular structure of the coefficients depended on a distance between the crystal and metal film; this fact has been experimentally confirmed.

Substantial changes of spatial light waves were also observed in crystals with imbedded metal nanoparticles [30–32]. In this case, optical phenomena were initiated by localised (not propagating) plasmons.

Phenomena observed in the interaction of plasmons with various nanostructured objects are indicative of the complexity of problems in this field.

In the present work we consider a rather simple and efficient scheme of plasmon interaction with plane waves. The simplest microstructured object is investigated, namely, a one-dimensional photonic crystal placed on a metal substrate. The dielectric function of the crystal is assumed periodic in the direction parallel to the input plane onto which the primary light wave falls. In this scheme the wave transformation at the crystal–metal interface can be described analytically and the intensity of the generated surface wave can be quantitatively estimated as a function of the primary wave intensity and the modulation period of the photonic crystal.

T.I. Kuznetsova, N.A. Raspopov P.N. Lebedev Physics Institute, Russian Academy of Sciences, Leninsky prosp. 53, 119991 Moscow, Russia; e-mail: tkuzn@sci.lebedev.ru, rna@sci.lebedev.ru

Received 2 March 2015; revision received 19 June 2015
Kvantovaya Elektronika **45** (11) 1055–1062 (2015)
Translated by N.A. Raspopov

2. Problem formulation

Consider a photonic crystal unlimited in the coordinates x and y. The plane $z = 0$ is the crystal–metal interface; the plane $z = -d$, onto which the primary radiation falls, is the crystal–air interface (Fig. 1). The alternating white and grey areas in Fig. 1 tentatively show a periodic dependence of the dielectric function on the coordinate. The spatial modulation of the dielectric function is generally described by an infinite set of Fourier harmonics. In this section we will estimate Fourier coefficients for several lower harmonics. In final calculations we will restrict ourselves to a single harmonic and a constant component. The dielectric function is taken in the form

$$\varepsilon = \varepsilon_0 + \tilde{\varepsilon}(e^{iGx} + e^{-iGx}). \quad (1)$$

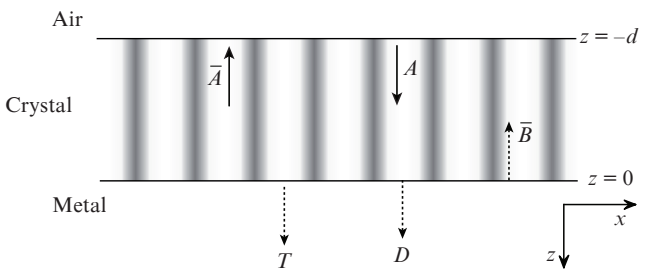

Figure 1. Waves at the photonic crystal–metal interface: $\bar{A}$ and A are the propagating waves in the crystal; $\bar{B}$ is the evanescent wave in the crystal; D, T are the evanescent waves in metal.

The magnetic permeability of the crystal is taken constant and equal to unity. In further calculations we will assume that an external source in the plane $z = -d$ produces the field $Ae^{-i\omega t}$, which is independent of y and x and propagates in the positive z-direction. We emphasise that the initial field propagates along the layers constituting the crystal. The situation differs, for example, from cases [16, 21] where the primary wave propagates perpendicular to the crystal layers.

For the numerical parameters of our problem we take characteristics of a synthetic opal (a 3D photonic crystal). Some parameters are taken from papers [33, 34] where nonlinear optical effects induced by radiation of a ruby laser (with the wavelength $\lambda = 2\pi c/\omega = 694.3$ nm) operating in the regime of giant oscillations have been studied. In these experiments, the convergence of the beam was usually about 0.1–0.05 rad. The average dielectric function is taken $\varepsilon_0 = 1.851$. This value corresponds to the case where pores between silica globules ($\varepsilon_{SiO_2} = 2.15$) are not filled ($\varepsilon_p = 1.0$).

The description of a real crystal requires a set of Fourier harmonics. In order to estimate the values of Fourier coefficients one may calculate these coefficients for several lower harmonics. Recall that the centres of spheres (silica globules) in a synthetic opal form the face-centred cubic structure.

Ideally, all globules are identical and described by a unique diameter D_{gl}, which is on the order of or less than 1 μm. In most cases D_{gl} varies from 200 to 700 nm. Consider the plane of the crystal in which centres of globules are arranged according to the hexagonal close packing (the plane 1, 1, 1). We draw in this plane axes x and y such that the x axis concatenates two nearest neighbouring globules, and the y axis is orthogonal to it. Let the z axis be orthogonal to the chosen plane. Obviously, the distance between the centres of the closest globules is $l_x = D_{gl}$ and the distance between neighbouring rows of globules is $l_y = D_{gl}\sqrt{3}/2$. The distance between neighbouring layers of globules is $l_z = D_{gl}\sqrt{2/3}$. The periods along the x, y and z axes are, respectively, $h_x = l_x$, $h_y = 2l_y$ and $h_z = 4l_z$. The corresponding wavenumbers are given by the expressions $G = 2\pi q/h_x$, $G' = 2\pi q'/h_y$, $G'' = 2\pi q''/h_z$, where q, q' and q'' are integers.

Consider the harmonic dependent on x only, that is, with the wavenumber of type $G = 2\pi q/h_x$. At $q = 1$ we obtain the Fourier coefficient equal to zero because the contributions from neighbouring rows of globules would compensate for each other. For second harmonic with the wavenumber $G = 4\pi/h_x$ the value of the Fourier coefficient is given by the expression

$$\tilde{\varepsilon}(G) = (\varepsilon_{sph} - \varepsilon_p) \times \frac{\iiint_{V_{N\,sph}} [\exp(iGx) + \exp(-iGx)]\,dx\,dy\,dz}{2\iiint_{V_{tot}} dx\,dy\,dz}. \quad (2)$$

Here, V_{tot} is the volume of a rectangular parallelepiped with the sides l_xN_x, l_yN_y, l_zN_z; $V_{N\,sph}$ is the volume of all N spheres ($N = N_xN_yN_z$) inside the volume V_{tot}; and ε_{sph} and ε_p are the dielectric constants of globules and pores, respectively. By expressing the numerator in terms of the sum of N equal integrals over a single sphere we finally obtain

$$\tilde{\varepsilon}(G) = (\varepsilon_{sph} - \varepsilon_p)\frac{\pi}{\sqrt{2}(GD_{gl}/2)^3} \times [\sin(GD_{gl}/2) - (GD_{gl}/2)\cos(GD_{gl}/2)]. \quad (3)$$

By substituting the values $G = 4\pi/h_x$, $h_x = D_{gl}$ into (3), we obtain $\tilde{\varepsilon} = 0.056(\varepsilon_{sph} - \varepsilon_p)$. Let us point out that the considered value of G corresponds to the period $D_{gl}/2$.

The Fourier coefficients for the wavenumbers dependent on y and z are calculated by a different scheme because of different phase relations between the contributions from neighbouring rows and neighbouring layers of globules into the total result. For three lowest harmonics contributing into the dependence of ε on $\{x, y, z\}$, namely, for $\{G, G', G''\} = \{\pi 4/D_{gl}, \pi 4/D_{gl}\sqrt{3}, \pi\sqrt{6}/D_{gl}\}$, we obtain the following values of the modulation component $\tilde{\varepsilon} = (\varepsilon_{sph} - \varepsilon_p)\{0.056, 0.064, 0.089\}$. To the chosen values of wavenumbers correspond the following values of modulation periods: $\{L, L', L''\} = \{D_{gl}/2, D_{gl}\sqrt{3}/2, D_{gl}\sqrt{2/3}\}$. By using the contrast of the dielectric function defined above through the values of ε for spheres and pores $\varepsilon_{sph} - \varepsilon_p = \varepsilon_{SiO_2} - \varepsilon_{air} = 1.15$, we can write the three values of the modulation coefficient in the form $\tilde{\varepsilon} = \{0.065, 0.073, 0.102\}$. In further calculations we will only retain the first coefficient adopting in this way the one-dimensional model of the photonic crystal. Let us introduce the ratio ξ of this coefficient to the average value of the dielectric function

$$\xi = \tilde{\varepsilon}(G)/\varepsilon_0. \quad (4)$$

At $\tilde{\varepsilon} = 0.065$ and $\varepsilon_0 = 1.851$ we have $\tilde{\varepsilon}/\varepsilon_0 = 0.035$. Note that the following condition holds

$$\xi \ll 1. \quad (5)$$

The smallness of the parameter ξ simplifies further calculations.

3. Eigenwaves in an unlimited photonic crystal

Consider the wave equation for a nonuniform medium (see [35]). In solving the problem it is reasonable to deal with transverse-magnetic (TM) waves and write out the magnetic field equations from [35] in the form

$$\Delta \boldsymbol{H} + \varepsilon \frac{\omega^2}{c^2}\boldsymbol{H} + \frac{1}{\varepsilon}[\nabla\varepsilon \times \mathrm{rot}\boldsymbol{H}] = 0. \tag{6}$$

The expression for the y-component of the magnetic field inside the crystal is taken in the form

$$H_y \equiv H = \mathcal{H}(x)\exp[\mathrm{i}k_z z];$$

hereafter, the time-dependent factor $\exp[-\mathrm{i}\omega t]$ is omitted. By writing Eqn (6) for the chosen spatial dependence of the field and taking into account properties (1) and (5) of the dielectric function ε, we obtain

$$\Delta H + \varepsilon_0 \frac{\omega^2}{c^2}H + \tilde{\varepsilon}\frac{\omega^2}{c^2}(\mathrm{e}^{\mathrm{i}Gx} + \mathrm{e}^{-\mathrm{i}Gx})H - \frac{1}{\varepsilon_0}\frac{\partial\varepsilon}{\partial x}\frac{\partial H}{\partial x} = 0. \tag{7}$$

In view of smallness of the parametera $\xi = \tilde{\varepsilon}/\varepsilon_0$, the field can be written as

$$H = (H_0 + H_1\mathrm{e}^{\mathrm{i}Gx} + H_{-1}\mathrm{e}^{-\mathrm{i}Gx})\mathrm{e}^{\mathrm{i}k_z z}. \tag{8}$$

Let us combine a system of equations for coupled waves as it is usually done in analysing waves in periodic structures (see [36, 37]). It is pertinent to note that in our case both the scattered waves included in (8) (H_1 and H_{-1}) are well off the Bragg resonance condition. Hence, neither of them is preferable and both should be taken into account on equal terms. Expression (7) entails the system of equations for three amplitudes H_0, H_1 and H_{-1}:

$$\begin{gathered}\left(\varepsilon_0\frac{\omega^2}{c^2} - k_z^2\right)H_0 + \xi\left(\varepsilon_0\frac{\omega^2}{c^2} - G^2\right)(H_1 + H_{-1}) = 0,\\ \xi\varepsilon_0\frac{\omega^2}{c^2}H_0 + \left(\varepsilon_0\frac{\omega^2}{c^2} - G^2 - k_z^2\right)H_j = 0,\ \ j = \pm 1.\end{gathered} \tag{9}$$

From (9), by setting the determinant equal to zero we obtain the third-order equation for the squared component of the wave vector k_z^2:

$$\begin{aligned}&\left(\varepsilon_0\frac{\omega^2}{c^2} - k_z^2\right)\left(\varepsilon_0\frac{\omega^2}{c^2} - k_z^2 - G^2\right)^2 - 2\xi^2\varepsilon_0\frac{\omega^2}{c^2}\\ &\times\left(\varepsilon_0\frac{\omega^2}{c^2} - G^2\right)\left(\varepsilon_0\frac{\omega^2}{c^2} - k_z^2 - G^2\right) = 0.\end{aligned} \tag{10}$$

One can easily obtain the expressions for three roots of k_z^2:

$$(k_z^2)_0 = \varepsilon_0\frac{\omega^2}{c^2} - \frac{G^2}{2} + \sqrt{\left(\frac{G^2}{2}\right)^2 - 2\xi^2\varepsilon_0\frac{\omega^2}{c^2}\left(G^2 - \varepsilon_0\frac{\omega^2}{c^2}\right)} \equiv k_0^2, \tag{11}$$

$$(k_z^2)_1 = \varepsilon_0\frac{\omega^2}{c^2} - \frac{G^2}{2} - \sqrt{\left(\frac{G^2}{2}\right)^2 - 2\xi^2\varepsilon_0\frac{\omega^2}{c^2}\left(G^2 - \varepsilon_0\frac{\omega^2}{c^2}\right)} \equiv -(\gamma_1)^2, \tag{12}$$

$$(k_z^2)_2 = \varepsilon_0\frac{\omega^2}{c^2} - G^2 \equiv -(\gamma_2)^2. \tag{13}$$

From exact formulae (11) and (12) one can easily obtain the simplified expressions for square wave vectors (with subscripts 0 and 1):

$$(k_z^2)_0 = \varepsilon_0\frac{\omega^2}{c^2} - 2\xi^2\varepsilon_0\frac{\omega^2}{c^2}\frac{G^2 - \varepsilon_0\omega^2/c^2}{G^2} \equiv k_0^2, \tag{14}$$

$$(k_z^2)_1 = \varepsilon_0\frac{\omega^2}{c^2} - G^2 + 2\xi^2\varepsilon_0\frac{\omega^2}{c^2}\frac{G^2 - \varepsilon_0\omega^2/c^2}{G^2} \equiv -(\gamma_1)^2. \tag{15}$$

The fields corresponding to the found eigenwave numbers are described by the formulae:

$$f_0(x,z) = \left[1 + \xi_{1,0}(\mathrm{e}^{\mathrm{i}Gx} + \mathrm{e}^{-\mathrm{i}Gx})\right]\mathrm{e}^{\mathrm{i}k_0 z} \tag{16}$$

for mode 0,

$$f_1(x,z) = \left[2\xi_{0,1} + (\mathrm{e}^{\mathrm{i}Gx} + \mathrm{e}^{-\mathrm{i}Gx})\right]\mathrm{e}^{-\gamma_1 z} \tag{17}$$

for mode 1, and

$$f_2(x,z) = (\mathrm{e}^{\mathrm{i}Gx} - \mathrm{e}^{-\mathrm{i}Gx})\mathrm{e}^{-\gamma_2 z} \tag{18}$$

for mode 2. Here we used the notations

$$\xi_{1,0} = \xi\frac{\varepsilon_0\omega^2/c^2}{G^2}, \qquad \xi_{0,1} = \xi\frac{G^2 - \varepsilon_0\omega^2/c^2}{G^2}. \tag{19}$$

The solution with subscript 2 is rejected because it yields the amplitudes $H_1 = -H_{-1}$, $H_0 = 0$; however, we will only consider the solutions that are symmetric in x.

It worth noting that for each of the modes (16) and (17) there is a corresponding inverted mode obtained by making the substitutions $k_0 \to -k_0$, $\gamma_1 \to -\gamma_1$:

$$\bar{f}_0(x,z) = f_0(x,-z),\ \ \bar{f}_1(x,z) = f_1(x,-z). \tag{20}$$

It should be stressed that the fields f_0 and f_1 do not interact in an infinitely long crystal. These waves only get coupled due to the boundary effect.

4. Wave transformation at the crystal–metal interface

The boundary conditions at the crystal-metal interface are expressed as

$$H\big|_{z=-0} = H\big|_{z=+0}, \tag{21}$$

$$\frac{1}{\varepsilon}\frac{\partial H}{\partial z}\bigg|_{z=-0} = \frac{1}{\varepsilon_{\rm m}}\frac{\partial H}{\partial z}\bigg|_{z=+0}, \tag{22}$$

where $\varepsilon_{\rm m}$ is the dielectric function of metal. The boundary conditions require taking into account the crystal modes $f_0(x,z)$, $\bar{f}_0(x,z)$ and $\bar{f}_1(x,z)$ as well as the metal modes with the x-components of the wave vector equal to 0, $\pm G$. In the general case, the total field inside the crystal is given by

$$H(x,z<0) = Af_0(x,z) + \bar{A}\bar{f}_0(x,z) + \bar{B}\bar{f}_1(x,z). \tag{23}$$

The field inside metal has the form

$$H(x,z>0) = T\exp(-\gamma_{\rm m}z) + D\exp(-\gamma_{\rm m,1}z)(e^{iGx} + e^{-iGx}), \tag{24}$$

where

$$\gamma_{\rm m} = \sqrt{-\varepsilon_{\rm m}\omega^2/c^2}, \quad \gamma_{\rm m,1} = \sqrt{G^2 - \varepsilon_{\rm m}\omega^2/c^2}\,. \tag{25}$$

By substituting expressions (23) and (24) into the boundary conditions (21), (22) and separating oscillating summands from those independent of x we obtain a system of equations for the amplitudes $A, \bar{A}, \bar{B}, T, D$. Solving the system it is possible to express all the amplitudes in terms of the amplitude A of the input wave. The system of equations for the unknown amplitudes can be written in the form

$$A + \bar{A} + \bar{B}2\xi_{0,1} = T, \tag{26}$$

$$(A + \bar{A})\xi_{1,0} + \bar{B} = D, \tag{27}$$

$$\frac{1}{\varepsilon_0}ik_0(A - \bar{A}) + \frac{1}{\varepsilon_0}\gamma_1\bar{B}2(\xi_{0,1} - \xi) = -\frac{1}{\varepsilon_{\rm m}}\gamma_{\rm m}T, \tag{28}$$

$$\frac{1}{\varepsilon_0}ik_0(A - \bar{A})(\xi_{1,0} - \xi) + \frac{1}{\varepsilon_0}\gamma_1\bar{B} = -\frac{1}{\varepsilon_{\rm m}}\gamma_{\rm m,1}D. \tag{29}$$

From (26)–(29) one can derive the expression for the coefficient of transformation of the initial wave into the surface wave:

$$\frac{\bar{B}}{A} = i2\xi\frac{k_0}{\varepsilon_0\varepsilon_{\rm m}}\frac{\nu\gamma_{\rm m,1} + \gamma_{\rm m}(1-\nu)}{(\gamma_{\rm m,1}/\varepsilon_{\rm m} + \gamma_1/\varepsilon_0)(\gamma_{\rm m}/\varepsilon_{\rm m} - ik_0/\varepsilon_0) + \delta}, \tag{30}$$

with the notations

$$\delta = 2\xi^2\Big[\nu\frac{\gamma_1}{\varepsilon_0} - (1-\nu)\frac{\gamma_{\rm m}}{\varepsilon_{\rm m}}\Big]\Big[\nu\frac{\gamma_{\rm m,1}}{\varepsilon_{\rm m}} + (1-\nu)\frac{ik_0}{\varepsilon_0}\Big]; \tag{31}$$

$$\nu = \frac{\varepsilon_0\omega^2/c^2}{G^2} \equiv \frac{\xi_{1,0}}{\xi}. \tag{32}$$

Expression (30) can be simplified if we neglect terms of the order of ξ^2. This is made by dropping δ in the denominator and excluding the small values proportional to ξ^2 in formulae (14) and (15) for the parameters k_0 and γ_1:

$$\frac{\bar{B}}{A} = i2\xi\frac{k_0}{\varepsilon_0\varepsilon_{\rm m}}\frac{\nu\gamma_{\rm m,1} + \gamma_{\rm m}(1-\nu)}{(\gamma_{\rm m,1}/\varepsilon_{\rm m} + \gamma_1/\varepsilon_0)(\gamma_{\rm m}/\varepsilon_{\rm m} - ik_0/\varepsilon_0)}, \tag{33}$$

$$(k_0)^2 = \varepsilon_0\omega^2/c^2, \quad -(\gamma_1)^2 = \varepsilon_0\omega^2/c^2 - G^2. \tag{34}$$

Note that the denominator of expression (33) for the surface wave amplitude comprises the factor

$$\gamma_{\rm m,1}/\varepsilon_{\rm m} + \gamma_1/\varepsilon_0, \tag{35}$$

which, after neglecting the terms of the order of ξ^2, takes the form

$$\frac{1}{\varepsilon_{\rm m}}\sqrt{G^2 - \varepsilon_{\rm m}\frac{\omega^2}{c^2}} + \frac{1}{\varepsilon_0}\sqrt{G^2 - \varepsilon_0\frac{\omega^2}{c^2}}\,. \tag{36}$$

One can see that expression (36) is a well-known formula used in plasmonics for calculating the wave vector of the surface plasmon. The wave vector of the plasmon is obtained (see [1]) by solving the equation

$$\frac{1}{\varepsilon_{\rm m}}\sqrt{K^2 - \varepsilon_{\rm m}\frac{\omega^2}{c^2}} + \frac{1}{\varepsilon_0}\sqrt{K^2 - \varepsilon_0\frac{\omega^2}{c^2}} = 0. \tag{37}$$

Expression (36) coincides with the left-hand side of (37) up to notations. The only distinction is that in our case the value of G is a purely real number whereas the solution of Eqn (37) for plasmons K is, generally, a complex number. Thus, one may assume that in a vicinity of plasmon resonance the surface wave amplitude may take an enhanced value. In the next Section we will search for a maximal modulus of expression (30) that determines the surface wave amplitude $\bar{B}$ relative to the initial wave amplitude A. In a numerical simulation we will vary the value of G in a vicinity of K_0 [i.e., the root of Eqn (37)].

5. Transformation of an nitial wave to a surface wave

The amplitude ratio $\bar{B}/A$ can be found by solving the system of equations (26)–(29). Let us determine the value of G corresponding to the maximal ratio $\bar{B}/A$. First, we consider the resonance factor in the denominator of (33) and find the condition of its turning to zero. Upon solving (37) with the complex parameter $\varepsilon_{\rm m}$ we obtain a complex root K_0. In our case, the Fourier harmonics of the dielectric function may only have real wave numbers. We take the real part of K_0 and put $G = {\rm Re}(K_0)$. Here we will consider only positive values of ${\rm Re}(K_0)$. The case of ${\rm Re}(-K_0)$ corresponds to an oppositely directed surface wave and may be considered in a similar way.

Recall that we consider the case of ruby laser radiation (λ = 694.3 nm) and the spatially averaged permittivity of the medium is $\varepsilon_0 = 1.851$. Let the adjoint metal be gold; at the radiation wavelength of the ruby laser, the dielectric function for gold is $\varepsilon_{\rm m} = -16.082 + 1.059i$. (Data on dielectric functions of metals were taken from [38].) A solution of Eqn (37) is $K_0 = (1.4458 + 0.00616i)\omega/c$. In view of the equality $G = {\rm Re}(K_0)$ we have $G = 1.4458\omega/c$. By substituting the value of G into (30) we obtain $\bar{B}/A = -0.687 + 1.599i$ and for the modulus of this ratio we have $|\bar{B}/A| = 1.741$. Thus, the amplitude of the surface wave is almost twice that of the initial propagating

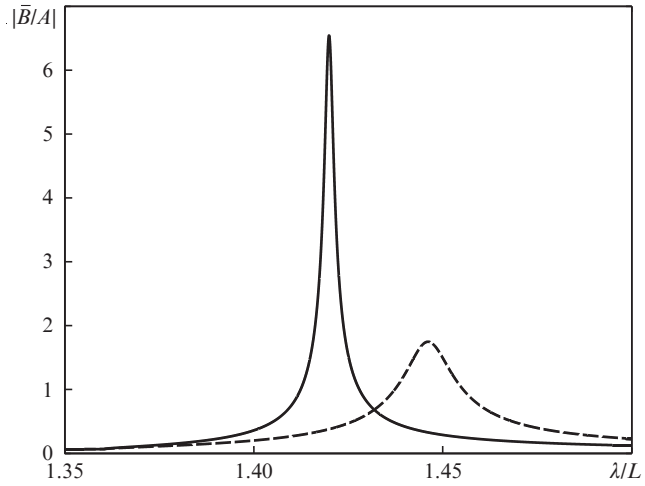

Figure 2. Efficiency of exciting a surface wave vs. the ratio of the radiation wavelength λ to the modulation period of the crystal dielectric function L for the cases of gold (dashed curve) and silver (solid curve) substrate.

wave. The maximal value of $\bar{B}/A$ can be found from calculations for a series of G values in a vicinity of the selected value $G = \mathrm{Re}(K_0)$. The dashed curve in Fig. 2 shows the dependence of $\bar{B}/A$ on the wave number G found from (30). One can see that the position of the actual maximum $G = 1.4461\omega/c$ is negligibly shifted from the above discussed value $G = 1.4458\omega/c$. This value of G corresponds to the period of the dielectric function modulation $L = 480$ nm. The maximal value of $\bar{B}/A$ is 1.742.

Similar calculations have been performed for silver as a metal adjoint to the photonic crystal. At the chosen radiation wavelength, the dielectric function of silver is $\varepsilon_m = -22.637 + 0.401\mathrm{i}$. The other system parameters remain unchanged. Due to small dissipation of silver, one may expect a more efficient excitation of the surface wave than in the case of gold. By performing calculations we obtain the complex value $K_0 = (1.4198 + 0.0011\mathrm{i})\omega/c$. Again, we put $G = \mathrm{Re}(K_0) = 1.4198\omega/c$. With this value of G we find from (30) $\bar{B}/A = -2.532 + 5.969\mathrm{i}$, and for the modulus of this value we have $|\bar{B}/A| = 6.483$. Thus, the surface wave amplitude in this case is almost 6.5 times that of the incident wave, that is, the transformation efficiency is more pronounced than in the case of gold.

By varying G in a vicinity of $G = \mathrm{Re}(K_0)$ we obtain the dependence of $|\bar{B}/A|$ on the wavenumber G, which is shown in Fig. 2. One can see that the position of the actual maximum $G = 1.4199\omega/c$ corresponding to the modulation period $L = 489$ nm is negligibly shifted along the G axis and the maximal value is $|\bar{B}/A| = 6.525$, which slightly differs from the starting value of 6.483. Hence, the estimates made by the approximate formulae are sufficiently accurate.

6. Tuning resonance curves

The characteristics of surface waves calculated in Section 5 testify the one-to-one correspondence between the radiation frequency and the photonic crystal period, which ensures the optimal excitation of plasmons. The method suggested implies that for a particular radiation frequency, the photonic crystal period (and the corresponding wavenumber G) should be accurately chosen. Nevertheless, minor changes in the scheme help overcome this difficulty. It would suffice to transfer to the inclined incidence of radiation onto a crystal. If the initial wave on a crystal surface has the form $\exp[\mathrm{i}(\omega/c)\times \sin\theta]$, then the satellite waves will arise with the wavenumbers $(\omega/c)\sin\theta \pm G$. Thus, the inclined incidence of radiation is equivalent to a change in the crystal period. In the case of inclined incidence, the system of equations (26)–(29) is not valid, and the calculation technique should be accordingly modified. For this purpose, one can use the approach elaborated in [39] and generalise it to our problem. The corresponding calculated efficiency of transformation of the inclined propagating wave to the surface wave is presented in Fig. 3.

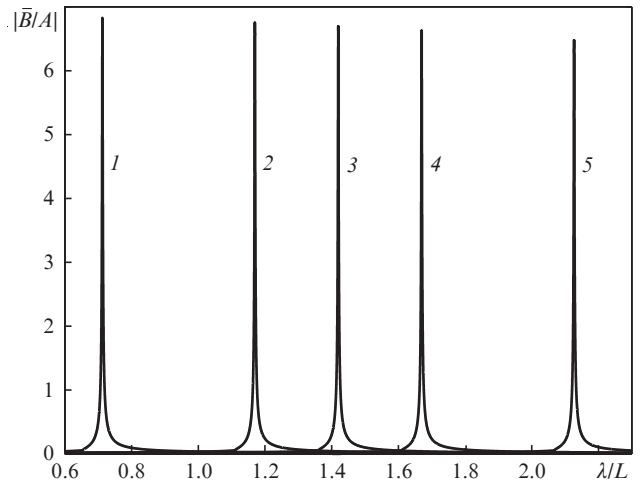

Figure 3. Efficiency of the initial wave-to-surface wave transformation at various incident angles θ in the case of a silver substrate: $\sin\theta = (1)$ 0.707, (2) 0.25, (3) 0, (4) –0.25, (5) –0.707.

The efficiency is shown versus the wavenumber of the Fourier harmonic of the dielectric function. Curves in Fig. 3 for various angles of incidence θ are similar in shape; however, they have different positions on the x axis (due to different G). The maxima of curves (1), (2), (3), (4) and (5) correspond to the modulation periods $L = 975$, 594, 489, 416 and 327 nm, respectively. A thorough calculation shows that the shapes of the curves are not absolutely identical and the difference may become quite noticeable at other values of numerical parameters; this especially concerns such a parameter as the contrast of the dielectric function. Note that low-intensity plasmons can be generated in a wide range of radiation frequencies and angles of incidence of the initial wave. The calculations performed in this section were aimed at finding the conditions for plasmons of elevated intensity. This requires a thorough matching of the crystal period with the angle of incidence of the initial wave.

7. Exit of the evanescent wave from the crystal to open space

Consider the exit of the surface wave outside the photonic crystal and subsequent wave propagation in a free space. It is necessary to consider one more crystal boundary; in our scheme, a side wall is placed in the plane $x = 0$. Rigorous consideration of this configuration and the corresponding changes in the field characteristics require a special analysis. The side boundary may noticeably distort the field structure,

which otherwise would exist in the crystal unlimited in the x direction. Similar problems were studied in our previous works devoted to the theoretical description of the spatial structure of light waves in nanowaveguides and to consideration of localised plasmons on the aperture of the channel in a metal layer [40–43]. It was shown that the exit plane generates reflected waves, which affect the spatial characteristics of the field that would exist if there were no boundary. Here we limit ourselves to a rough solution assuming that the field inside the crystal–metal system is not affected by the side boundary. In addition, in the undisturbed field we only retain the most intensive part of the field and neglect weak components. Thus, the field in the exit plane takes the form

$$H_y(x=0, z\leqslant 0) = A\exp(\mathrm{i}k_0 z) + \bar{A}\exp(-\mathrm{i}k_0 z) + \bar{B}\exp(\gamma_1 z), \tag{38}$$

$$H_y(x=0, z>0) = T\exp(-\gamma_m z) + D\exp(-\gamma_{m,1} z). \tag{39}$$

First we consider two propagating waves: the initial wave with amplitude A and the corresponding oncoming wave with amplitude $\bar{A}$. The jump of the dielectric function on the side boundary (from $\varepsilon_0 = 1.851$ to $\varepsilon_{out} = 1$) provides for these waves the condition of total internal reflection. Note that in both cases of normal incidence onto the upper plane and of inclined incidence (when the angle of incidence is not too large $0 \leqslant \theta \leqslant 42°$) the wave is locked inside the crystal. Therefore, it is reasonable to exclude the contribution of the waves with amplitudes A and $\bar{A}$ from field calculation in free space.

Consider the contribution of surface waves to the field structure in free space. In contrast to the waves A and $\bar{A}$, the evanescent wave propagating in the positive x direction weakly reflects from the side boundary. Due to a large modulus of the wave vector G, the side boundary scarcely prevents the plasmon from exiting outside.

Concerning the contribution of evanescent waves it worth noting that near the resonance in the case considered in Section 5 the following estimates for the amplitudes are valid: $|T| \leqslant \xi|\bar{B}|$, $|D-\bar{B}| \approx \xi|\bar{B}|$. In view of these estimates, we may neglect the amplitude T and substitute D for $\bar{B}$ in our calculations.

In free space, it is easy to calculate the field structure produced by the surface wave exiting through the plane $x = 0$. By rejecting in (38) the propagating waves, the surface wave passing to the negative x direction, and the waves that make a small contribution to the field in the region $x \geqslant 0$, we arrive at the following expression for calculating the external field

$$\begin{aligned} H_{exit}(x=0, z\leqslant 0) &= \bar{B}\exp(\gamma_1 z), \\ H_{exit}(x=0, z>0) &= \bar{B}\exp(-\gamma_{m,1} z). \end{aligned} \tag{40}$$

By expanding the function H_{exit} in Fourier series, continuously extending it to $x > 0$, and assuming there are no waves coming to the plane $x = 0$ from the side of positive x values, we obtain the equality

$$H_{out}(x,z) = \frac{1}{2\pi}\int_{-\infty}^{\infty}\int_{-\infty}^{\infty} H_{exit}(z') \times \exp\left[\mathrm{i}\eta(z-z') + \mathrm{i}x\sqrt{\frac{\omega^2}{c^2}-\eta^2}\right]\mathrm{d}\eta\,\mathrm{d}z'. \tag{41}$$

By substituting expression (40) for the field in the exit plane to formula (41), we obtain

$$H_{out}(x,z) = \frac{1}{2\pi}\int_{-\infty}^{\infty}\exp\left(\mathrm{i}\eta z + \mathrm{i}x\sqrt{\frac{\omega^2}{c^2}-\eta^2}\right) \times\left(\frac{1}{\gamma_1 - \mathrm{i}\eta} + \frac{1}{\gamma_{m,1} + \mathrm{i}\eta}\right)\mathrm{d}\eta. \tag{42}$$

At long distances from exit plane we have $x\omega/c \gg 1$, and for z satisfying the condition $|z|\gamma_1 \ll x\omega/c$, from the obtained expression we find the absolute value of the field

$$H_{max}(x,z) = \frac{1/\gamma_1 + 1/|\gamma_{m,1}|}{\sqrt{x\lambda}}, \tag{43}$$

which is maximal for a given x = const. Thus, the field amplitude falls inversely proportional to the square root of the distance between the exit plane and observation point. Numerical calculations have been performed for a wide range of coordinates x and z by formula (42).

The following parameters characterising the field in the exit plane were used: for gold $\gamma_1 = 0.49\omega/c$, $|\gamma_{m,1}| = 4.26\omega/c$; for silver $\gamma_1 = 0.39\omega/c$, $|\gamma_{m,1}| = 4.96\omega/c$. Dimensionless constant $\bar{B}$ was taken equal to unity. Contour plots of the absolute value of field in external space ($x > 0$) are shown in Fig. 4. The crystal was placed in the spatial range of negative values of z, the metal was placed below the crystal, similarly to the scheme presented earlier in Fig. 1. At point $x = 0$, $z = 0$ the value of field equals unity. In Fig. 4 one can see, that greater intensity values are shifted towards negative z values. One can also see that the wave amplitude decreases with x according to the estimate made above.

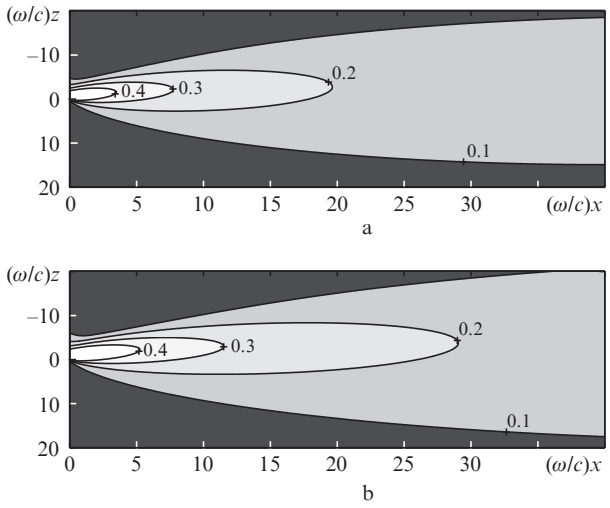

Figure 4. Distribution of the absolute value of the field in external space in the cases of (a) gold and (b) silver substrates.

8. Conclusions

The expressions for the eigenwaves excited in a one-dimensional photonic crystal by an initial wave directed parallel to crystal layers have been found. A transverse structure of the eigenwaves comprises a constant and an oscillating component. Among the eigenwaves obtained there are evanescent waves with a transverse structure comprising a strong oscillating component and a weak constant component. Frequencies of these waves are beyond forbidden photonic zones. The propagating eigenwaves have a weak oscillating component and a strong constant component. If the crystal has a boundary with a metal substrate, the evanescent waves transform into plasmons. The system of equations is derived, which describes redistribution of electromagnetic energy over waves at the interface with a metal substrate. Formula for calculating the ratio of the plasmon amplitude to the amplitude of the initial wave has been obtained.

It has been shown that the amplitude of the evanescent wave may be on the order of or even exceed (at particular parameters) the amplitude of the propagating wave. The evanescent wave is most intensive when system parameters are close to the conditions of plasmon resonance.

The expressions for eigenwaves used in the present work clearly demonstrate that the surface plasmon propagates along the crystal–metal interface with zero exponential attenuation. The undamped regime is provided by the primary wave coming onto the crystal from an external source.

Thus, the scheme suggested provides a simple way for exciting surface plasmons.

Particular attention has been paid to the problem of emergence of electromagnetic radiation to open space through a side boundary. It is evident that in the considered scheme with adopted impedance values, a plasmon freely escapes to outer space. However, the value of the permittivity jump at the crystal–air interface is sufficient to ensure the total internal reflection for the initial propagating wave. This wave leaks to outer space only to a distance on the order of a light wavelength.

Thus, the exit of a plasmon to free space is not accompanied by noticeable background. When the surface wave exits through the lateral wall to open space, the radiation field propagates similarly to the field of a two-dimensional localised source. Therefore, the spatial dependence of the field amplitude is inversely proportional to the square root of the distance to an observation point.

Efficient generation of surface plasmons in the considered scheme requires that the radiation frequency be exactly matched with the photonic crystal period. The required period should provide the plasmon resonance condition. If the radiation frequency is not resonant for a particular crystal then the scheme can be modified. It is easy to tune the scheme by varying the angle of incidence of initial radiation onto the crystal surface.

Acknowledgements. This work was partly supported by the Russian Foundation for Basic Research (Grant No 15-02-07777-a) and the Physical Sciences Division of the Russian Academy of Sciences (Fundamental Optical Spectroscopy and Its Applications Programme).

References

1. Raether H. *Surface Plasmons on Smooth and Rough Surfaces and on Gratings* (Berlin: Springer, 1988).
2. Laluet J.-Y., Drezet A., Genet C., Ebbesen T.W. *New J. Phys*., **10**, 105014 (2008).
3. Baudrion A.-L., de Leon-Perez F., Mahbaub O., Hohenau A., Ditlbacher H., Garcia-Vidal F.J., Dintinger J., Ebbesen T.W., Martin-Moreno L., Krenn J.R. *Opt. Express*, **16**, 3420 (2008).
4. Kihm H.W., Lee K.G., Kim D.S., Ahn K.J. *Opt. Commun*., **282**, 2442 (2009).
5. Dai W., Soukoulis C.M. *Phys. Rev. B*, **80**, 155407 (2009).
6. Nikitin A.Yu., Rodrigo S.G., Garcia-Vidal F.J., Martin-Moreno L. *New J. Phys*., **11**, 123020 (2009).
7. Nikitin A.Yu., Garcia-Vidal F.J., Martin-Moreno L. *Phys. Stat. Sol. RRL*, **4**, 250 (2010).
8. Han Z., Bozhevolnyi S.I. *Rep. Prog. Phys*., **76**, 016402 (2013).
9. Ebbesen T.W., Lezec H.J., Chaemi H.F., Thio T., Wolff P.A. *Nature*, **391**, 667 (1998).
10. Chang S.H., Gray S.K., Shatz G.C. *Opt. Express*, **13**, 3150 (2005).
11. de Abajo G.F.J., Sáenz J.J., Dolado J.S. *Opt. Lett*., **14**, 7 (2006).
12. Ebbesen T.W., Degiron A. *Pure Appl. Opt*., **7**, S90 (2005).
13. Joannopoulos J.D., Johnson S.G., Winn J.N., Meade R.D. *Photonic Crystals, Molding the Flow of Light* (New York: Princeton Univ. Press, 2008).
14. Romanov S.G., Korovin A.V., Regensburger A., Peschel U. *Adv. Mater*., **23**, 2515 (2011).
15. Massaro A. (Ed.). *Photonic Crystals – Innovative Systems, Lasers and Waveguides* (Rijeka, Croatia: InTech, 2012).
16. Kuzmiak V., Maradudin A.A. *Phys. Rev. B*, **55**, 7427 (1997).
17. Meade R.D., Brommer K.D., Rappe A.M., Joannopoulos J.D. *Phys. Rev. B*, **44**, 10961 (1991).
18. Barnes W.L., Dereux A., Ebbesen T.W. *Nature*, **424**, 01937 (2003).
19. Gaspar-Armenta J., Villa F. *J. Opt. Soc. Am. B*, **20**, 2349 (2003).
20. Ramirez-Duverger A.S., Gaspar-Armenta J., Garcia-Llamas R. *J. Opt. Soc. Am. B*, **25**, 1016 (2008).
21. Hajian H., Soltan-Vala A., Kalafi M. *Opt. Commun*., **292**, 149 (2013).
22. Konopsky V.N., Alieva E.V. *Phys. Rev. Lett*., **97**, 253904 (2006).
23. Konopsky V.N., Alieva E.V. *Opt. Lett*., **34**, 479 (2009).
24. Romanov S.G., Vogel N., Bley K., Landfester K., Weiss C.K., Orlov S., Korovin A.V., Chuiko G.P., Regensburger A., Romanova A.S., Kriesch A., Peschel U. *Phys. Rev. B*, **86**, 195145 (2012).
25. Ding B., Pemble M.E., Korovin A.V., Peschel U., Romanov S.G. *Phys. Rev. B*, **82**, 035119 (2010).
26. Gaspar-Armenta J., Villa F. *J. Opt. Soc. Am. B*, **30**, 2271 (2013).
27. Romanov S.G., Regensburger A., Korovin A.V., Romanova A.S., Peschel U. *Phys. Rev. B*, **88**, 125418 (2013).
28. Romanov S.G., Peschel U., Bardosova M., Essig S., Busch K. *Phys. Rev. B*, **82**, 115403 (2010).
29. Ding B., Bardosova M., Pemble M.E., Korovin A.V., Peschel U., Romanov S.G. *Adv. Funct. Mater*., **21**, 4182 (2011).
30. Barth M., Schietinger S., Fischer S., Becker J., Nusse N., Aichele T., Lochel B., Sonnichsen C., Benson O. *Nano Lett*., **10**, 891 (2010).
31. Hasan D., Wang A.X. *Proc. SPIE Int. Soc. Opt. Eng.*, **8632**, 863203 (2013).
32. Mukherjee I., Gordon R. *Opt. Express*, **20**, 16992 (2012).
33. Tcherniega N.V., Kudryavtseva A.D. *J. Russ. Laser Res.*, **27**, 450 (2006).

34. Gorelik V.S., Kudryavtseva A.D., Tareeva M.V., Tcherniega N.V. *Pis'ma Zh. Eksp. Teor. Fiz.*, **84**, 575 (2006) [*JETP Lett*., **84**, 485 (2006)].
35. Landau L.D., Lifshits E.M. *Electrodynamics of Continuous Media* (New York: Pergamon Press, 1963; Moscow: Nauka, 1982).
36. Ziman J. *Principles of the Theory of Solids* (Cambridge: Cambridge University Press, 1972; Moscow: Mir, 1974).
37. Yariv A., Yeh P. *Optical Waves in Crystals* (New York: Wiley, 1984; Moscow: Mir, 1987).
38. Palik E.D. *Handbook of Optical Constants of Solids* (New York: Academic, 1985).
39. Kuznetsova T.I. *J. Russ. Laser Res*., **34**, 63 (2013).
40. Kuznetsova T.I., Lebedev V.S. *Phys. Rev. E*, **78**, 016607 (2008).
41. Kuznetsova T.I., Lebedev V.S. *Phys. Rev. B*, **70**, 035107 (2004).
42. Kuznetsova T.I., Lebedev V.S., Tsvelik A.M. *J. Opt. A, Pure Appl. Opt*., **6**, 338 (2004).
43. Kuznetsova T.I., Raspopov N.A. *Kvantovaya Elektron*., **42**, 87 (2012) [*Quantum Electron*., **42**, 87 (2012)].